Improvement in District Scale Heavy Rainfall Prediction Over Complex Terrain of North East India Using Deep Learning

Omveer Sharma, *Member, IEEE*, Dhananjay Trivedi, Sandeep Pattnaik, Vivekananda Hazra, and Niladri B. Puhan, *Member, IEEE*

***Abstract*— Predicting heavy rainfall events (HREs) in real-time poses a significant challenge in India, particularly in complex terrain regions like Assam, where these hydro-meteorological events are frequently associated with flash floods with severe consequences over the region. The devastating HREs in June 2022 led to numerous casualties, extensive damage, and economic losses exceeding 200 crores, necessitating the evacuation of over 4 million individuals. Even recently, June 2023, Assam went through immense flooding situation. Due to the limitations of deterministic numerical weather models in accurately forecasting these events, the study explores the incorporation of deep learning (DL) models, specifically U-Nets, using simulated daily accumulated rainfall outputs from various parameterization schemes. Over a four-day period in June 2022, the U-Net-based model demonstrated superior skills in predicting rainfall at the district scale, achieving a mean absolute error (MAE) of less than 12 mm, outperforming individual and ensemble model outputs. Comparing the DL model's performance to the weather research and forecasting (WRF) forecasts, it exhibited a remarkable 64.78% reduction in MAE across Assam. Notably, the proposed model accurately predicted HREs in specific districts such as Barpeta, Kamrup, Kokrajhar, and Nalbari, showcasing improved spatial variation compared with the WRF model. The DL model's predictions aligned with actual rainfall (>150 mm) observations from the India Meteorological Department (IMD), while the WRF forecasts consistently underestimated rainfall intensity (<100 mm). Furthermore, the proposed model achieved a high prediction accuracy of 77.9% in categorical rainfall prediction, significantly outperforming the WRF schemes by 38.1%.**

***Index Terms*— Deep learning (DL), heavy rainfall prediction, rainfall prediction, U-Net.**

I. Introduction

HEAVY rainfall event (HRE) and the ensuing flooding have had a considerable detrimental impact on human society in terms of property destruction and human life losses. HRE can occur anywhere; however, some places are more prone to it than others [1]. Mountainous places are more likely to undergo excessive rainfall and flooding due to geography or orographic impacts. Northeast India (NEI) is surrounded by mountains to the north, east, and south along with lesser ranges inside the area, with only opening to west to receive precipitation carried by westerlies. The southwest-monsoon causes heavy rainfall over the NEI region. Monsoon 2022 arrived in NEI in the final week of May or the first week of June.

Due to the distinctive physical features of the area and the increased frequency of such HREs, flash floods connected to extreme rain events are major hydrological disasters in the NEI including Assam regions. The climatological study done by Mahanta et al. [2] over the NEI region shows the decreasing trend of convective available potential energy (CAPE) between the study period, and the increasing trend of convective inhibition energy (CIN) represents that CAPE is not the only factor responsible for HREs. Extreme rainfall and very deep convective episodes are caused by strong updrafts brought on by gravity waves within the mesoscale organization [3]. Despite possessing certain universal traits, these violent convective storms are specific to each place because local factors such as topography and ground hydrology have a big impact on how the systems form and develop.

Heavy rainfall prediction is a highly intricate, multiscale process; operational agencies find it challenging to forecast with sufficient foresight. These severe rainfall events have traditionally been predicted using numerical weather prediction (NWP). Convective parameterization, microphysics, and planetary boundary layer parameterization are used in NWP models to depict the clouds and precipitation processes to predict rainfall [4], [5], [6]. The prediction of precipitation and related factors depends heavily on these parameterizations. Microphysics can be used at high resolutions (1–3 km) to explicitly resolve the convective precipitation without the need of convective methods. Several studies using weather research and forecasting–advance research WRF (WRF-ARW) for heavy rainfall prediction over Chennai, Korea, and Italy have been done [7], [8], [9]. All these deterministic models, however, struggle to accurately forecast rainfall in terms of its evolution, amount, distribution, and severity, especially at the district scale with sufficient lead time, where most of the policy and disaster response measures are undertaken in real-time.

Even while the NWP models are generally good at predicting HRE, the traditional approach occasionally produces

Manuscript received 30 June 2023; revised 5 September 2023; accepted 4 October 2023. Date of publication 9 October 2023; date of current version 23 October 2023. This work was supported in part by the New Venture Fund, USA; in part by the Indian Institute of Technology Bhubaneswar; and in part by the Council of Scientific and Industrial Research. *(Corresponding author: Sandeep Pattnaik.)*

Omveer Sharma, Dhananjay Trivedi, Sandeep Pattnaik, and Vivekananda Hazra are with the School of Earth Ocean and Climate Sciences, Indian Institute of Technology Bhubaneswar, Bhubaneswar 752050, India (e-mail: os10@iitbbs.ac.in; a21es09005@iitbbs.ac.in; spt@iitbbs.ac.in; vh15@iitbbs.ac.in).

Niladri B. Puhan is with the School of Electrical Sciences, Indian Institute of Technology Bhubaneswar, Bhubaneswar 752050, India (e-mail: nbpuhan@iitbbs.ac.in).

This article has supplementary downloadable material available at https://doi.org/10.1109/TGRS.2023.3322676, provided by the authors.

Digital Object Identifier 10.1109/TGRS.2023.3322676

erratic results regarding the frequency and intensity of HREs. Recently, there has been an increase in interest in using artificial intelligence (AI) to forecast the weather and other climatic variables. A neural network was created by Goswami and Srividya [10] to forecast rainfall across the Indian subcontinent. Error backpropagation technique was used by Venkatesan et al. [11] to forecast rainfall during the Indian summer monsoon. Sahai et al. [12] used artificial neural network (ANN) techniques to predict the rainfall associated with the Indian summer monsoon. For predicting the annual rainfall across China, Wang and Sheng [13] suggested a generalization regression neural network (GRNN). The hourly rainfall in Bangkok was predicted by Hung et al. [14] using a generalized feedforward neural network. Deng et al. [15] used the U-Net model to forecast summer precipitation in China. The study demonstrated that on average, the utilization of U-Net led to a significant reduction in the root-mean-square error of the original CFSv2 prediction. Wang et al. [16] proposed the utilization of machine learning (ML) classification models to predict the locations of storm cells. In addition, ML regression models were recalibrated using relevant predictors and combined with the ML classification models. This integration aimed to facilitate early warnings of HREs. Over the Indian region, the prediction of Indian summer monsoon rainfall through deep learning (DL) and stacked decoder and autoencoder-based regression model shows significant improvement [17], [18].

To the best of our knowledge, no studies have been conducted to forecast rainfall location, amount, and intensities at the district scale of the complex terrain states over the Assam region using DL models using forecast outputs from high-resolution weather models. This region is highly vulnerable to floods associated with heavy rainfall frequently (i.e., 2022, 2023). In addition, the majority of earlier research relied on observational or reanalysis data, both of which have relatively limited real-world implications. Our study aims to improve forecast skills for rainfall prediction with a lead time in terms of intensity at the district level with two DL models named as U-Net with and without residual connection. Finally, the best approach has been implemented to enhance the forecast at the district scale. The major contributions of the research are outlined below.

1) *Unexplored Territory:* No previous studies have used DL models to forecast rainfall at the district scale in the complex terrain of the Assam region. This research fills this gap using DL models with high-resolution weather model outputs.
2) *Flood Vulnerability:* The Assam region is highly prone to floods caused by heavy rainfall, occurring frequently in recent years. By focusing on improving rainfall prediction accuracy and lead time at the district level, this research aims to enhance flood preparedness and mitigation strategies.
3) *Practical Forecast Enhancement:* Unlike previous research relying on limited data sources, this study aims to bridge the gap between research and real-world applications. By implementing two DL models, namely, U-Net with and without residual connection, the research enhances the accuracy and reliability of rainfall forecasts, providing valuable insights for decision-makers and resource management at the district scale.

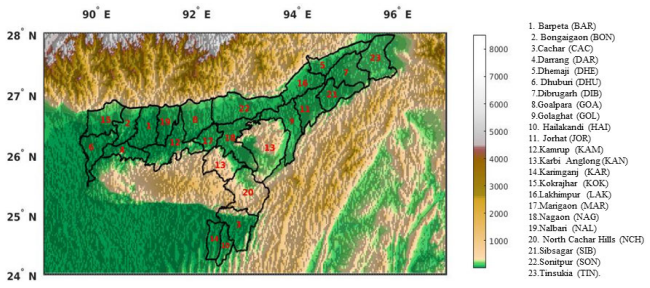

Fig. 1. Districtwise Assam topographical map.

In summary, the research contributes by introducing DL models for district-scale rainfall prediction in the Assam region, addressing flood vulnerability, and improving practical applications of rainfall forecasts. The rest of this article is organized as follows. Section II presents data and methodology. The results and discussion are described in Section III. Finally, the conclusion is made in Section IV.

II. Data and Methodology

A. Study Area

Assam, a state in northeastern India, is located on the south of the Eastern Himalayas. Assam is 78 438 km^2 in size and is situated between latitudes 24° 08′N and 28° 02′N and longitudes 89° 42′E and 96° 00′E (Fig. 1). Large-scale flood plains are created in this area because of the considerable rainfall that the rivers Brahmaputra, Barak, and their tributaries get virtually all year long. With an average annual rainfall of roughly 1140 cm, the majority of it comes from the southwest monsoon. The study area is home to numerous species and true tropical rainforests.

In June 2022, Assam alone received 669 mm of rainfall, 61% more than the usual 415.2 mm, according to the statewise data from India Meteorological Department (IMD). Kokrajhar district receives the highest rainfall in June and July in Assam, as shown by the 30 year's IMD data. The district receives 757 mm of rainfall in June, 714 mm in July, and 561 mm in August, while Chirang district receives the most rainfall in September (456 mm). The least amount of rainfall occurs in Karbi district. Here, we are going to investigate one of the HREs that occurred in Assam between 15 and 19 June 2022. According to a bulletin from Central Water Commission, as of June 17, eight rivers were flowing above the high flood level and three rivers were flowing above the danger level. In the event days, landslides have also been reported in Dima-Hasao, Morigaon, and Kamrup. In the state, landslides and flooding have claimed the lives of 80 individuals while over 40 lakh people were adversely affected. Assam's economy suffers from floods severely as a result, losing an estimated $200 million.

B. Data

HREs over Assam between 15 and 19 June 2022 have been simulated at a horizontal resolution of 3 km and lead time up to Day 4 (96 h) using the weather research and

TABLE I
WRF 4.2.1 MODEL CONFIGURATION DETAILS

Options	Parent Domain	Inner Domain
Horizontal Resolution	15 km	5
Vertical Levels	35	35
Forecast Length	96 hour	96 hour
Time Step	30 s	10 s
Model Forecast Output Time Interval	6 hourly	3 hourly
Planetary Boundary Layer	ACM, BOU, MRF, MYN, QNS, YSU	
Microphysics	AAT, GOD, MOR, THOM, WDM7, WSM7	
Long-wave Radiation Short-wave Radiation	CAM [19]	
Surface Layer	MM5 Similarity scheme [20]	
Land Surface	Unified Noah land-surface model [21]	
Land Use and Land Surface Datasets	1. USGS and 2. ISRO	
Cumulus	CUTR, CU2, CU5, CU6, CU11, CU93	Explicitly resolved
SST(daily): ERA5 [22] Initial and Boundary conditions (6 hourly): ERA5 [22]		

forecast (WRF-4.2, [23]) advanced version, which is a non-hydrostatic state-of-the-art mesoscale NWP model. A total of 44 cases have been taken, out of which 18 runs including six runs of different cumulus convection parameterization, cloud microphysics parameterization, and planetary boundary layer parameterization with United States Geological Survey (USGS) land use land cover (LULC). Similarly, 18 cases of the same configuration but Indian Space Research Organization (ISRO) LULC are simulated. In addition, eight cases are ensembles of aforementioned parameterization schemes, and LULC experiments are also used for this study. However, for testing purpose we have used ensemble eight cases to validate with IMD, and DL model outputs as ensemble forecast are superior to any deterministic forecasts. A detailed description is provided in Table I. The daily accumulated rainfall at the district level of Assam has been taken as input in the DL model.

To provide better rainfall estimates over land and water, observational rain gauge data are coupled with data from the global precipitation measurement (GPM) microwave imager and dual-frequency precipitation radar [24] with a spatial resolution of $0.25° \times 0.25°$ and a temporal resolution of a daily basis. Bilinear interpolation has been carried out to downscale 25-km IMD data to 3-km resolution to match with WRF forecast outputs at the district scale. The WRF dataset contains 4048 district-level daily accumulated rainfall samples and it is randomly divided into the training and testing datasets with a ratio of 80% and 20%, respectively. The 2706 samples are used to train our architecture, and the remaining dataset (testing data) is used to evaluate the performance of the proposed architecture which contains 1342 samples.

C. Methodology

The primary component of the model used in this study was the U-Net model. The U-Net architecture has demonstrated excellent performance in weather prediction and postprocessing tasks [25]. The U-Net model is a deep neural network known for its fully symmetric encoding–decoding structure. Its

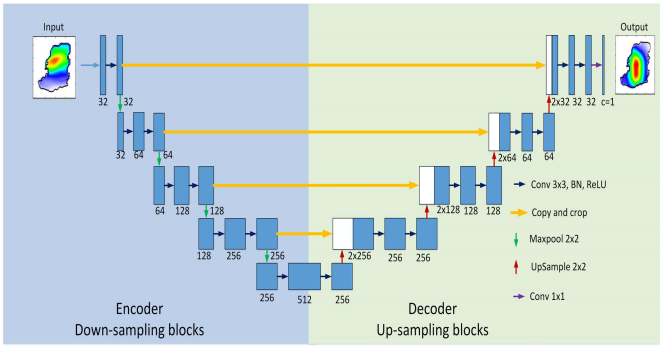

Fig. 2. U-Net architecture is illustrated in the diagram. Arrows symbolize the distinct operations, blue boxes depict the feature maps at each layer, and white boxes represent the cropped feature maps obtained from the contracting path.

encoder compresses features, while the decoder reconstructs them. In contrast to the original U-Net, which had four downsampling and four upsampling blocks, the U-Net model used in this study consisted of three levels to decrease model complexity and mitigate overfitting (see Fig. 2). As previously mentioned, the U-Net can be divided into two parts. The first part is the contracting path, which adopts a typical convolution neural network (CNN) architecture [26]. Each block in this path consists of two consecutive 3×3 convolutions, followed by a ReLU activation unit and a max-pooling layer. This arrangement is repeated multiple times. The novelty of the U-Net lies in its second part, known as the expansive path. In this path, each stage upsamples the feature map using 2×2 upconvolution. Then, the corresponding layer's feature map from the contracting path is cropped and concatenated with the upsampled feature map. Two successive 3×3 convolutions and ReLU activation are then applied. In the final stage, a 1×1 convolution is added to reduce the feature map to the desired number of channels and generate the segmented image. The overall U-Net architecture is depicted in Fig. 2. In the U-Net architecture, a modification has been made by incorporating a residual connection between two consecutive convolution layers. As a result, this study uses two U-Net-based models. The first model, denoted as U-Net ($-$R), does not include a residual connection, whereas the second model, denoted as U-Net ($+$R), incorporates a residual connection.

In our approach, we used a batch size of 64, an initial learning rate of 0.0001, and implemented early stopping with a patience of 20 epochs. This strategy aimed to prevent overfitting by halting training if there was no improvement in the loss function on the validation dataset. To further optimize the training process, we used a learning rate scheduler. Specifically, the learning rate decreased by a factor of 0.1 after every ten epochs without any improvement in the validation loss.

III. RESULTS AND DISCUSSION

In this section, we will conduct a thorough analysis and discussion of the rainfall forecasting abilities attributable to outcomes from deterministic WRF models and from DL

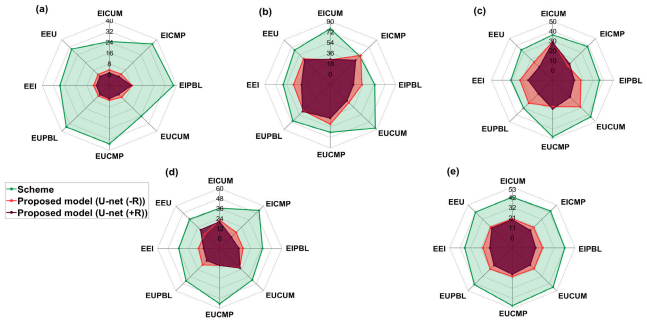

Fig. 3. Daywise Spyder plot over all districts for all ensemble schemes, i.e., EICUM, EICMP, EIPBL, EUCUM, EUCMP, EUPBL, EEI, and EEU with U-Net model with residual connection and U-Net model without residual connection for (a) Day 1, (b) Day 2, (c) Day 3, (d) Day 4, and (e) all days.

TABLE II
EXPERIMENTAL DESIGN

S. No.	Experiment Name	Details of the Experiment
1	ISRO-LULC	Ensemble (EICMP) : mean of 6 members of Microphysics (MP) Ensemble (EICUM) : mean of 6 members of Cumulus Physics (CU) Ensemble (EIPBL) : mean of 6 members of Planetary Boundary Layer (PBL) Ensemble (EEI) : mean of all schemes (EICMP, EICUM, EIPBL)
2	USGS-LULC	Ensemble (EUCMP) : mean of 6 members of Microphysics (MP) Ensemble (EUCUM) : mean of 6 members of Cumulus Physics (CU) Ensemble (EUPBL) : mean of 6 members of Planetary Boundary Layer (PBL) Ensemble (EEU) : mean of all schemes (EUCMP, EUCUM, EUPBL)

model at the district scale of Assam. Our proposed model outperforms all the parameterization schemes of WRF and their ensemble to predict the rainfall at district scale of Assam. We describe the experiments in great depth and test the results against the benchmark models in Sections III-A–III-C.

A. Daywise Assessment

The performance of our proposed models, U-Net (−R) and U-Net (+R), is evaluated and compared with the deterministic WRF model. Fig. 3(a)–(e) illustrates the daywise accumulated rainfall mean absolute error (MAE) for all the districts of Assam, considering various ensembles of WRF parameterization schemes as mentioned in Table II (i.e., EICUM, EICMP, EIPBL, EUCUM, EUCMP, EUPBL, EEI, and EEU), as well as the U-Net models, in relation to the observed IMD rainfall.

On Day 1, the EUCUM demonstrates the lowest MAE (24.2 mm), followed by EICUM (24.5 mm), EEI (27.2 mm), and EEU (33.1 mm), while the highest MAE is noted for EIPBL (37.8 mm) [Fig. 3(a)]. In contrast, our proposed U-Net models, both U-Net (−R) and U-Net (+R), consistently achieve significantly lower MAE (<8 mm) compared with the other ensembles. On Day 2, there is a subsequent increase in MAE values, with the highest value noted for the EUCUM (86.6) for all the districts of Assam. Among the ensembles, the EICMP exhibits the lowest error (50.6) [Fig. 3(b)]. Comparatively, the U-Net models outperform the ensemble, showcasing MAE values ranging from 24 to 36 mm, except for the EICMP.

The MAE for all the ensembles on Day 3 ranges between 30 and 40 mm, with the exception of EUCUM (42.9 mm) and EUCMP (47.7 mm) [Fig. 3(c)]. The decrease in MAE on Day 3 indicates improved performance of the deterministic model compared with Day 2, and this might be due to model spin up. The U-Net (−R) exhibits higher MAE than the U-Net (+R).

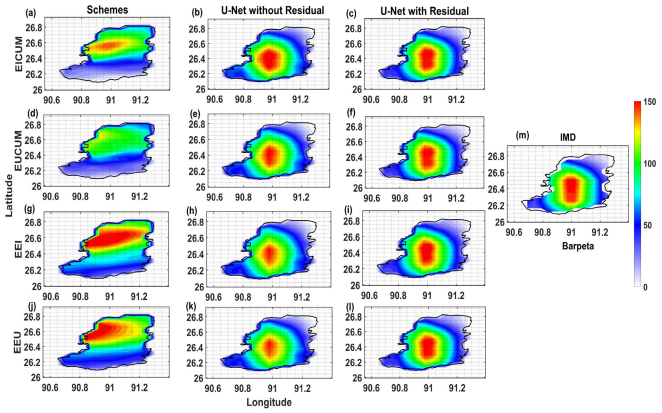

Fig. 4. Contour plot of Day 1 accumulated rainfall for Barpeta district for ensemble scheme with their respective U-Net models output and IMD (m). Schemes (First column), U-Net without residual (Second column), U-Net with residual (third column). (a), (b), and (c)EICUM. (d), (e), and (f) EUCUM. (g), (h), and (i) EEI. (j), (k), and (l) EEU.

With the exception of the EICUM, the U-Net (+R) reduces the MAE to a range of 10–20 mm, indicating an increase in prediction skill for heavy rainfall [Fig. 3(c)].On the final day (Day 4) of the model simulation, the EEI exhibits the lowest MAE (35.4 mm), indicating that the ensemble of all the ISRO LULC and parameterization schemes performs well compared with USGS ensembles [Fig. 3(d)]. However, the U-Net (+R) model further improves the rainfall prediction and reduces the MAE to less than 12 mm for the same scheme. In addition, the U-Net (−R) model also enhances forecast accuracy with an MAE of less than 24 mm across all the districts. When considering the performance across all the days, the WRF forecast shows that the EEI is the best with an MAE of 33.6 mm, followed by EEU (42.33 mm). The U-Net models outperform all the forecast outputs and provide rainfall predictions that closely match the observed (IMD), with an MAE of less than 24 mm [Fig. 3(e)]. Particularly, the U-Net (+R) model demonstrates an even lower MAE of less than 20 mm, thereby improving the forecast accuracy. Furthermore, MAE, root mean square error (RMSE), and mean percentage error (MPE) for different ensemble schemes and the proposed models are presented in Table S1 (in the supplementary).

B. Districtwise Heavy Rainfall Prediction

Figs. 4–7 present the districtwise contour plots illustrating the districts that are most susceptible to HRE on different days. For validation purposes, the ensembles of schemes with the least MAE across all the districts in Assam are chosen from Fig. 3. Among these schemes, EICUM, EUCUM, EEI, and EEU exhibited the lowest MAE of 24.5, 24.2, 27.2, and 33.1 mm, respectively. Specifically, according to IMD, Barpeta experienced heavy rainfall in Day 1. The EUCUM, which demonstrated the lowest MAE, depicted 100 mm of rainfall in the northern region of Barpeta and less than 50 mm of rainfall in the southern region [Fig. 4(d)]. The U-Net (+R) [Fig. 4(f)] exhibited a broader coverage with rainfall intensity of 150 mm, matching the rainfall variation as observed by IMD [Fig. 4(m)]. The EICUM [Fig. 4(a)] illustrated rainfall intensities ranging from 100 to 125 mm in the northwest area

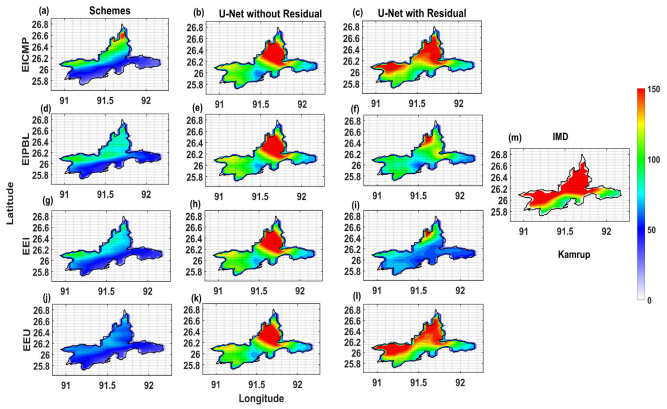

Fig. 5. Contour plot of Day 1 accumulated rainfall for Kamrup district for ensemble scheme with their respective U-Net models output and IMD (m). Schemes (First column), U-Net without residual (Second column), U-Net with residual (third column). (a), (b), and (c) EICMP. (d), (e), and (f) EIPBL. (g), (h), and (i) EEI. (j), (k), and (l) EEU.

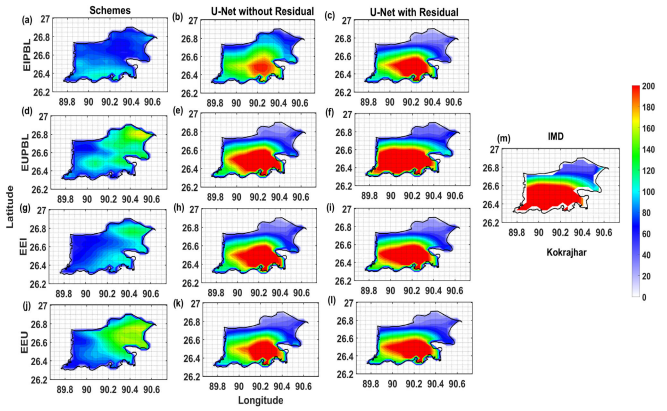

Fig. 6. Contour plot of Day 1 accumulated rainfall for Kokrajhar district for ensemble scheme with their respective U-Net models output and IMD (m). Schemes (First column), U-Net without residual (Second column), U-Net with residual (third column). (a), (b), and (c) EIPBL. (d), (e), and (f) EUPBL. (g), (h), and (i) EEI. (j), (k), and (l) EEU.

of Barpeta, while the EEI [Fig. 4(g)] and EEU [Fig. 4(j)] significantly overestimated rainfall, exceeding 150 mm in the upper Barpeta district. However, both the U-Net models, U-Net(−R) & U-Net(+R), displayed similar rainfall intensity (150 mm) in central Barpeta, gradually decreasing in line with IMD observations. For the EICUM, EUCUM, EEI, and EEU, the respective average MAEs are 48.2, 44.5, 50.2, and 48.6 mm for accumulated rainfall in Barpeta district. However, when using U-Net (−R), the MAE for the same schemes is 7.9, 7.9, 8.5, and 10.1 mm, respectively. On the other hand, when using U-Net (+R), the MAE significantly decreases to 2.3, 2.0, 2.2, and 2.3 mm, respectively. These results clearly demonstrate a notable enhancement in rainfall prediction accuracy using DL models.

On Day 2, Kamrup district had heavy rainfall (>150 mm) in the north and over 100 mm in the south, as per IMD [Fig. 5(m)]. To validate our models, we selected schemes with the lowest MAE across Assam's districts: EICMP (50.6 mm), EIPBL (55 mm), EEI (59.5 mm), and EEU (65.2 mm). These schemes performed best for Day 2 in the deterministic model. EICMP, with the lowest MAE, underestimated rainfall in the northern Kamrup (<100 mm) and southern regions (<50 mm) [Fig. 5(a)]. The U-Net (−R) model captured rainfall intensity

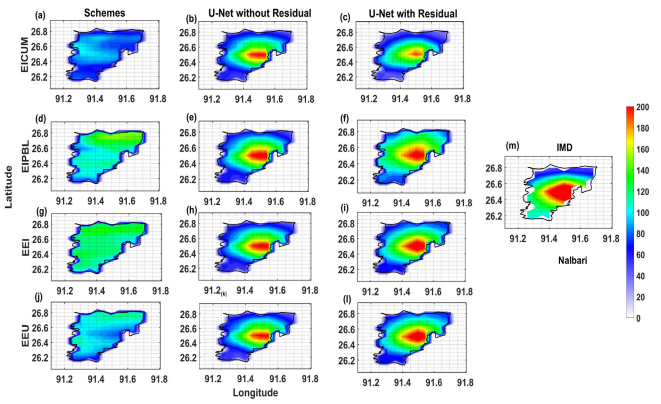

Fig. 7. Contour plot of Day 1 accumulated rainfall for Nalbari district for ensemble scheme with their respective U-Net models output and IMD (m). Schemes (First column), U-Net without residual (Second column), U-Net with residual (third column). (a), (b), and (c) EICUM. (d), (e), and (f) EIPBL. (g), (h), and (i) EEI. (j), (k), and (l) EEU.

in the north but underestimated it in the west [Fig. 5(k)]. The U-Net (+R) model accurately captured daily rainfall variability throughout the district [Fig. 5(l)]. EEU showed very little rainfall (<40 mm) over the district [Fig. 5(j)], but the U-Net (−R) model significantly improved rainfall estimation, especially in the northern Kamrup (>140 mm) [Fig. 5(k)]. The U-Net (+R) model performed well, accurately capturing rainfall intensity across the district [Fig. 5(l)]. For EIPBL [Fig. 5(d)] and EEI [Fig. 5(g)], which underestimated rainfall to a lesser extent than EEU, the proposed U-Net (−R) model enhanced rainfall estimation. However, the U-Net (+R) model's performance was slightly inferior to the U-Net (−R) model. MAE for various ensemble schemes and the proposed model can be found in Table S2 (in the supplementary).

On Day 3, the events were highly devastating, with many Assam districts experiencing daily rainfall exceeding 200 mm. Accurately predicting such high-intensity rainfall was a major challenge for the deterministic model. Kokrajhar district was severely affected, with over 200 mm in the south, 100–150 mm in the middle, and 50 mm in the north [Fig. 6(m)]. EIPBL showed very little rainfall (<50 mm) across the district and failed to capture the high-intensity rainfall [Fig. 6(a)]. In contrast, both the proposed models significantly improved the spatial variations in daily rainfall [Fig. 6(b) and (c)]. EUPBL, EEI, and EEU also underestimated rainfall, with slight spatial variations [Fig. 6(d), (g), and (j)]. The results showed that U-Net (+R) [Fig. 6(f), (i), and (l)] outperformed U-Net (−R) [Fig. 6(e), (h), and (k)]. U-Net (+R) effectively captured highly accurate rainfall variability using EUPBL forecasts [Fig. 6(f)]. Contour plots for other districts such as Barpeta and Nalbari are shown in Figs. S1 and S2 (in the supplementary), yielding similar conclusions. MAE values for various ensemble schemes and the proposed model are given in Table S2 (in the supplementary).

On Day 4 of the event, Nalbari district experienced rainfall exceeding 200 mm. The central part of Nalbari received more rainfall compared with other areas. The EICUM exhibited very little rainfall (<50 mm) across the entire district and failed to capture the HRE [Fig. 7(a)]. However, both the proposed models, U-Net (−R) and U-Net

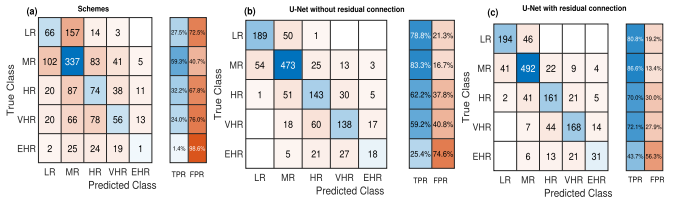

Fig. 8. Confusion matrix for all the WRF schemes (a) U-Net model without residual connection, (b) U-Net model with residual connection, and (c) for LR, MR, HR, VHR, and EHR classes.

(+R), are able to significantly improve the spatial variation in daily rainfall [Fig. 7(b) and (c)]. The EIPBL, EEI, and EEU also underestimated the magnitude of rainfall, but some light spatial variations with rainfall (>100 mm) are observed [Fig. 7(d), (g), and (j)]. Both the proposed models, U-Net (−R) and U-Net (+R), successfully captured these subtle spatial variations and generated a more accurate representation of HREs. The results demonstrated that U-Net (+R) [Fig. 7(f), (i), and (l)] outperformed U-Net (−R) [Fig. 7(e), (h), and (k)]. The proposed U-Net (+R) model provided highly accurate rainfall variability using the EEI output [Fig. 7(f)]. Table S2 presents the MAE values for various ensemble schemes and the proposed model.

C. Categorical Rainfall Prediction

To assess the performance of the proposed model, a total of 1342 samples are used in the testing phase. The rainfall categories across districts are classified based on the standard IMD criteria for daily rainfall thresholds: light rainfall (LR, 2.5–15 mm), moderate rainfall (MR, 15.6–64.5 mm), heavy rainfall (HR, 64.5–115.4 mm), very heavy rainfall (VHR, 115.5–204.4 mm), and extremely heavy rainfall (EHR, >204.5 mm), with different lead times (Day 1—24 h to Day 4—96 h). In the testing dataset, there were 240 samples belonging to LR, 568 samples belonging to MR, 230 samples belonging to HR, 233 samples belonging to VHR, and 71 samples belonging to EHR. These samples represented the output of different WRF experiments (Table I).

The overall performance of the schemes is evaluated using a confusion matrix, as shown in [Fig. 8(a)]. Out of the 240 LR samples, only 66 samples are correctly predicted. For the 568 MR samples, 337 samples are correctly predicted. In the case of 230 HR samples, only 74 samples were correctly predicted. Similarly, for 233 VHR samples, only 56 are correctly predicted, and for 71 EHR samples, only one is correctly predicted [Fig. 8(a)]. Consequently, the classification accuracies true positive rate (TPR) for LR, MR, HR, VHR, and EHR were 27.5%, 59.3%, 32.2%, 24%, and 1.4%, respectively. The overall accuracy is calculated to be 39.8%. These results indicate that all the WRF schemes performed poorly for HR, VHR, and EHR samples.

Using the WRF outputs, both the proposed models [U-Net (−R) and U-Net (+R)] provide more accurate categorical rainfall predictions, as shown in [Fig. 8(b) and (c)]. For U-Net (−R), out of 240 LR samples, 189 samples are correctly predicted. For 568 MR samples, 473 samples are correctly predicted. In the case of 230 HR samples, only 143 samples are correctly predicted. Similarly, for 233 VHR samples, only 138 are correctly predicted, and for 71 EHR samples, only 18 are correctly predicted [Fig. 8(b)]. This translates to classification accuracies of 78.8% for LR, 83.3% for MR, 62.2% for HR, 59.2% for VHR, and 25.4% for EHR. The overall accuracy is calculated to be 71.6%. Notably, the U-Net (−R) model shows improvement, particularly for the HR, VHR, and EHR rainfall categories.

In the case of U-Net (+R), further improvement is noted, especially for the HR, VHR, and EHR rainfall categories. Out of 240 LR samples, 194 samples are correctly predicted. For 568 MR samples, 492 samples are correctly predicted. For 230 HR samples, only 161 samples are correctly predicted. Similarly, for 233 VHR samples, only 168 are correctly predicted, and for 71 EHR samples, only 31 are correctly predicted [Fig. 8(c)]. The classification accuracies for LR, MR, HR, VHR, and EHR are 80.8%, 86.6%, 70%, 72.1%, and 43.7%, respectively. The overall accuracy for U-Net (+R) is 77.9%. These results demonstrate a highly significant improvement in categorical rainfall prediction accuracy. In addition, the proposed model shows enhanced capability in accurately classifying HREs.

As mentioned before, the schemes EICUM, EIPBL, EEI, and EEU consistently outperform other WRF schemes for all the days. The corresponding confusion matrices are shown in [Fig. 9(a)–(d)]. For the EICUM scheme, the TPR values for LR, MR, HR, VHR, and EHR are 0%, 73.7%, 30%, 0%, and 0%, respectively [Fig. 9(a)]. The proposed U-Net (−R) model performs better than the corresponding scheme, with TPR values of 75% for LR, 94.7% for MR, 50% for HR, 60% for VHR, and 66.7% for EHR [Fig. 9(e)]. In the case of U-Net (+R), the TPR values for LR, MR, HR, VHR, and EHR are 100%, 94.7%, 60%, 50%, and 66.7%, respectively [Fig. 9(i)].

In the case of the EIPBL scheme, the TPR values for LR, MR, HR, VHR, and EHR are 0%, 66.7%, 77.8%, 16.7%, and 0%, respectively [Fig. 9(b)]. The proposed U-Net (−R) model outperforms the corresponding scheme, achieving TPR values of 100% for LR, 87.5% for MR, 77.8% for HR, 58.3% for VHR, and 0% for EHR [Fig. 9(f)]. The U-Net (+R) model further improves the categorical rainfall prediction accuracy, with TPR values of 100% for LR, 95.8% for MR, 66.7% for HR, 91.7% for VHR, and 66.7% for EHR [Fig. 9(j)].

In the case of EEI, the TPR values for LR, MR, HR, VHR, and EHR are 10%, 82.4%, 80%, 33.3%, and 0%, respectively [Fig. 9(c)]. The proposed U-Net (−R) model performs better than the corresponding scheme, achieving TPR values of 80% for LR, 82.4% for MR, 60% for HR, 50% for VHR, and 33.3% for EHR [Fig. 9(g)]. The U-Net (+R) model further enhances the categorical rainfall prediction accuracy, with TPR values of 90% for LR, 94.1% for MR, 100% for HR, 66.7% for VHR, and 66.7% for EHR [Fig. 9(k)].

In the case of EEU, the TPR values for LR, MR, HR, VHR, and EHR are 0%, 70.6%, 33.3%, 18.2%, and 0%, respectively [Fig. 9(d)]. The proposed U-Net (−R) model outperforms the corresponding scheme, achieving TPR values of 83.3% for LR, 100% for MR, 66.7% for HR, 45.5% for VHR, and 0% for EHR [Fig. 9(h)]. The U-Net (+R) model further enhances the categorical rainfall prediction accuracy, with TPR values of 100% for LR, 100% for MR, 66.7% for HR, 63.6% for VHR, and 25% for EHR [Fig. 9(l)].

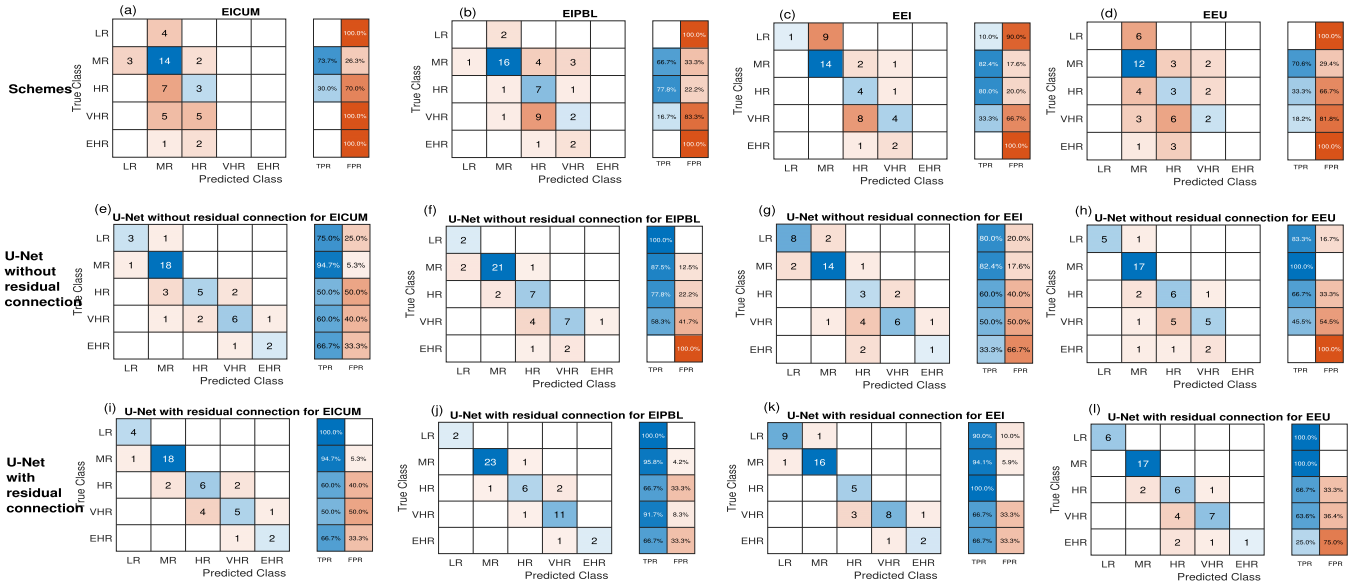

Fig. 9. (a)–(d) Confusion matrix for WRF schemes, (e)–(h) U-Net model without residual connection, and (i)–(l) U-Net model with residual connection for LR, MR, HR, VHR, and EHR classes.

Confusion matrices for the other four schemes, namely, EICMP, EUCUM, EUCMP, and EUPBL, can be found in Fig. S3(a)–(d). The performance of U-Net (−R) corresponding to these schemes is shown in Fig. S3(e)–(h), indicating improved accuracy in categorical rainfall prediction. In addition, further enhancement in prediction performance can be observed in Fig. S3(i)–(l) when using U-Net (+R). The effectiveness of both the proposed U-Net models in predicting HREs for all the four days is evident. They exhibit a significant improvement in capturing the spatial variability of HREs across districts compared with the WRF schemes. The results demonstrate the capability of the proposed models to accurately predict categorical rainfall throughout Assam. Moreover, the proposed models successfully capture and predict rare HREs in specific districts, showcasing high spatial accuracy. In general, the performance of U-Net (+R) surpasses that of U-Net (−R).

IV. Conclusion

This study conducted a thorough analysis and discussion of rainfall forecasting abilities using deterministic WRF models and a DL model at the district scale of Assam. The proposed DL model, U-Net, outperformed all the parameterization schemes of WRF and their ensemble in predicting rainfall at the district scale. The daywise assessment showed that the U-Net models consistently had lower MAE values compared with the WRF ensemble schemes, indicating better performance in rainfall prediction, and it exhibited a remarkable 64.78% reduction in MAE across Assam. The districtwise analysis revealed that the U-Net models captured the spatial variability of rainfall more accurately compared with the WRF schemes. The proposed architectures improved the prediction of HREs, and the U-Net model with a residual connection showed even better performance, reducing MAE values and improving forecast accuracy. In addition, the categorical rainfall prediction evaluation demonstrated that the WRF schemes performed poorly for moderate, heavy, very heavy, and extremely heavy rainfall categories. However, both the proposed U-Net models provided more accurate categorical rainfall predictions, with significant 38.1% improvements observed by achieving 77.9% prediction accuracy, particularly for HREs. Overall, the results of this study indicate that the proposed U-Net models are capable of enhancing district-level rainfall forecasting expertise in Assam, especially for HREs. These models outperformed the WRF schemes and demonstrated improved accuracy in capturing spatial and categorical rainfall variability. The findings of this research contribute to the advancement of rainfall prediction methods, which can have significant implications for disaster management and mitigation efforts in the region.

To further enhance and establish the proposed model's effectiveness and robustness, using a large dataset would be beneficial in the future work. By incorporating a substantial amount of data, the model can capture a wider range of patterns, relationships, and variations, resulting in more accurate and reliable heavy rainfall predictions.

References

[1] D. R. Easterling, J. Evans, P. Y. Groisman, T. R. Karl, K. E. Kunkel, and P. Ambenje, "Observed variability and trends in extreme climate events: A brief review," *Bull. Amer. Meteorol. Soc.*, vol. 81, no. 3, pp. 417–426, 2000.

[2] R. Mahanta, D. Sarma, and A. Choudhury, "Heavy rainfall occurrences in northeast India," *Int. J. Climatol.*, vol. 33, no. 6, pp. 1456–1469, May 2013.

[3] B. B. Goswami, P. Mukhopadhyay, R. Mahanta, and B. N. Goswami, "Multiscale interaction with topography and extreme rainfall events in the northeast Indian region," *J. Geophys. Res., Atmos.*, vol. 115, no. D12, 2010.

[4] V. Hazra and S. Pattnaik, "Influence of cloud microphysical parameterization on the characteristics of monsoon depressions over the Indian region," *Int. J. Climatol.*, vol. 41, no. 14, pp. 6415–6432, Nov. 2021.

[5] T. Chakraborty, S. Pattnaik, R. K. Jenamani, and H. Baisya, "Evaluating the performances of cloud microphysical parameterizations in WRF for the heavy rainfall event of Kerala (2018)," *Meteorol. Atmos. Phys.*, vol. 133, no. 3, pp. 707–737, Jun. 2021.

[6] D. Rai and S. Pattnaik, "Evaluation of WRF planetary boundary layer parameterization schemes for simulation of monsoon depressions over India," *Meteorol. Atmos. Phys.*, vol. 131, no. 5, pp. 1529–1548, Oct. 2019.

[7] S.-Y. Hong and J.-W. Lee, "Assessment of the WRF model in reproducing a flash-flood heavy rainfall event over Korea," *Atmos. Res.*, vol. 93, no. 4, pp. 818–831, Aug. 2009.

[8] P. R. Mohan, C. V. Srinivas, V. Yesubabu, R. Baskaran, and B. Venkatraman, "Simulation of a heavy rainfall event over Chennai in southeast India using WRF: Sensitivity to microphysics parameterization," *Atmos. Res.*, vol. 210, pp. 83–99, Sep. 2018.

[9] E. Avolio and S. Federico, "WRF simulations for a heavy rainfall event in southern italy: Verification and sensitivity tests," *Atmos. Res.*, vol. 209, pp. 14–35, Sep. 2018.

[10] P. Goswami and Srividya, "A novel neural network design for long range prediction of rainfall pattern," *Current Sci.*, vol. 70, no. 6, pp. 447–457, 1996.

[11] C. Venkatesan, S. D. Raskar, S. S. Tambe, B. D. Kulkarni, and R. N. Keshavamurty, "Prediction of all India summer monsoon rainfall using error-back-propagation neural networks," *Meteorol. Atmos. Phys.*, vol. 62, nos. 3–4, pp. 225–240, 1997.

[12] A. K. Sahai, M. K. Soman, and V. Satyan, "All India summer monsoon rainfall prediction using an artificial neural network," *Climate Dyn.*, vol. 16, no. 4, pp. 291–302, Apr. 2000.

[13] Z.-L. Wang and H.-H. Sheng, "Rainfall prediction using generalized regression neural network: case study Zhengzhou," in *Proc. Int. Conf. Comput. Inf. Sci.*, Dec. 2010, pp. 1265–1268.

[14] N. Q. Hung, M. S. Babel, S. Weesakul, and N. K. Tripathi, "An artificial neural network model for rainfall forecasting in Bangkok, Thailand," *Hydrol. Earth Syst. Sci.*, vol. 13, no. 8, pp. 1413–1425, Aug. 2009.

[15] Q. Deng, P. Lu, S. Zhao, and N. Yuan, "U-Net: A deep-learning method for improving summer precipitation forecasts in China," *Atmos. Ocean. Sci. Lett.*, vol. 16, no. 4, Jul. 2023, Art. no. 100322.

[16] Y. V. Wang et al., "Relative importance of radar variables for nowcasting heavy rainfall: A machine learning approach," *IEEE Trans. Geosci. Remote Sens.*, vol. 61, 2023, Art. no. 4100314.

[17] B. Kumar et al., "Deep learning based forecasting of Indian summer monsoon rainfall," *Algorithms*, vol. 9, no. 11, p. 13, 2021.

[18] M. Saha, A. Santara, P. Mitra, A. Chakraborty, and R. S. Nanjundiah, "Prediction of the Indian summer monsoon using a stacked autoencoder and ensemble regression model," *Int. J. Forecasting*, vol. 37, no. 1, pp. 58–71, Jan. 2021.

[19] W. D. Collins et al., "Description of the NCAR community atmosphere model (CAM 3.0)," Nat. Centre Atmos. Res. (NCAR), Boulder, CO, USA, NCAR Tech. Note NCAR/TN-464+STR, vol. 226, 2004, pp. 1326–1334.

[20] C. A. Paulson, "The mathematical representation of wind speed and temperature profiles in the unstable atmospheric surface layer," *J. Appl. Meteorol. Climatol.*, vol. 9, no. 6, pp. 857–861, Dec. 1970.

[21] N. M. Tewari et al., "Implementation and verification of the unified NOAH land surface model in the WRF model (Formerly Paper Number 17.5)," in *Proc. 20th Conf. Weather Anal. Forecasting/16th Conf. Numer. Weather Predict.*, Seattle, WA, USA, vol. 14, 2004.

[22] H. Hersbach et al., "The ERA5 global reanalysis," *Quart. J. Roy. Meteorol. Soc.*, vol. 146, no. 730, pp. 1999–2049, Jul. 2020.

[23] W. C. Skamarock et al., "A description of the advanced research WRF model version 4," Nat. Center Atmos. Res., Boulder, CO, USA, Tech. Rep., 2019, p. 550, vol. 145, no. 145.

[24] A. K. Mitra, A. K. Bohra, M. N. Rajeevan, and T. N. Krishnamurti, "Daily Indian precipitation analysis formed from a merge of rain-gauge data with the TRMM TMPA satellite-derived rainfall estimates," *Meteorol. J.*, vol. 87, pp. 265–279, 2009.

[25] J. A. Weyn, D. R. Durran, and R. Caruana, "Improving data-driven global weather prediction using deep convolutional neural networks on a cubed sphere," *J. Adv. Model. Earth Syst.*, vol. 12, no. 9, 2020, Art. no. e2020MS002109.

[26] O. Sharma, N. C. Sahoo, and N. B. Puhan, "Kernelized convolutional transformer network based driver behavior estimation for conflict resolution at unsignalized roundabout," *ISA Trans.*, vol. 133, pp. 13–28, Feb. 2023.

Omveer Sharma (Member, IEEE) received the Ph.D. degree from the Indian Institute of Technology (IIT) Bhubaneswar, Bhubaneswar, India, in 2023.

He is currently working as a Senior Research Fellow with the School of Earth Ocean and Climate Sciences, IIT Bhubaneswar. His research interests include deep learning (DL), machine learning (ML), biometrics, medical image analysis, advance vehicle control for autonomous vehicle, and intelligent decision-making.

Dhananjay Trivedi received the B.Sc. degree (Hons.) in mathematics, and the M.Sc. (Tech.) degree in geophysics from Banaras Hindu University, Varanasi, India, in 2017 and 2021, respectively.

Currently, he is working as a Ph.D. Scholar with the School of Earth Ocean and Climate Sciences, IIT Bhubaneswar, Bhubaneswar, India. He is currently working on tropical cyclones and extreme events over India.

Sandeep Pattnaik is an Associate Professor with the School of Earth Ocean and Climate Sciences, IIT Bhubaneswar, Bhubaneswar, India. He has published more than 60 research articles and guided many master's and Ph.D. students. His research interests include extreme weather modeling and forecast using high-resolution weather models.

Dr. Pattnaik was an Associate Fellow of Indian Meteorological Society, India.

Vivekananda Hazra received the B.Tech. degree in mechanical engineering from West Bengal University, Kolkata, India, in 2014, and the Ph.D. degree from the Indian Institute of Technology Bhubaneswar, Bhubaneswar, India, in 2023.

Currently, he is working as a Research Associate with IIT Bhubaneswar. He is currently working on monsoon low-pressure systems over India.

Niladri B. Puhan (Member, IEEE) received the B.E. degree in electrical engineering from UCE Burla, Burla, Odisha, India, in 2000, the M.E. degree in signal processing from the Indian Institute of Science, Bangalore, India, in 2002, and the Ph.D. degree from Nanyang Technological University, Singapore, in 2007.

He is currently an Assistant Professor with the School of Electrical Sciences, IIT Bhubaneswar, Bhubaneswar, India. His research interests include signal and image processing, biometrics, medical image analysis, and machine learning (ML).